Molecular phylogeny and ultrastructure of *Selenidium serpulae* (Apicomplexa, Archigregarinia) from the calcareous tubeworm *Serpula vermicularis* (Annelida, Polychaeta, Sabellida)

Brian S. Leander

Accepted: 23 November 2006
doi:10.1111/j.1463-6409.2007.00272.x

Leander, B. S. (2007). Molecular phylogeny and ultrastructure of *Selenidium serpulae* (Apicomplexa, Archigregarinia) from the calcareous tubeworm *Serpula vermicularis* (Annelida, Polychaeta, Sabellida). — *Zoologica Scripta*, *36*, 213–227.

Archigregarines are dynamic single-celled parasites that inhabit the intestinal systems of marine invertebrates, especially suspension feeding and deposit feeding polychaetes. Certain archigregarines in the genus *Selenidium* have retained several plesiomorphic characters, and improved knowledge of these species is expected to shed considerable light onto the earliest stages in apicomplexan evolution. Although archigregarines are related to some of the most notorious parasites known (e.g., *Cryptosporidium* and *Plasmodium*), current knowledge of the group is meagre. In an attempt to improve our understanding of archigregarine diversity and evolution, I have characterised the general ultrastructure and molecular phylogenetic position of *Selenidium serpulae* (Lankester) Caullery and Mesnil. The parasites were isolated from the intestines of the calcareous tubeworm *Serpula vermicularis* (Polychaeta) collected in the eastern Pacific Ocean. The trophozoites (extracellular feeding stages) were spindle-shaped and capable of slow and continuous bending, and coiling, especially when dislodged from the host epithelium. The trophozoite surface was composed of 19–23 longitudinal folds, prominent transverse folds and a robust, trilayered pellicle subtended by a single row of microtubules, each surrounded by an electron transparent sheath. Putative mitochondria were observed, but they were inconspicuous and apparently highly reduced, a condition that is indicative of anaerobic metabolism. The small subunit (SSU) rDNA sequence from *S. serpulae* was very closely related to two (short) sequences derived from an environmental PCR survey of an oxygen-depleted hydrothermal vent system in the Gulf of California, namely C1-E017 (AY046619) and C2-E016 (AY046806). This result suggested that archigregarines with a morphology and lifecycle much like that in *S. serpulae* are thriving in this oxygen poor ecosystem. In addition, phylogenetic analyses of a larger SSU rDNA dataset (excluding the shorter environmental sequences) indicated that the nearest sister lineage to *S. serpulae* was *S. vivax*, a bizarre tape-like gregarine found in the intestines of sipunculids. This relationship was bolstered by comparative ultrastructural data and helped to illustrate that the diversification and biogeographical distribution of archigregarine parasites is probably more extensive than usually assumed.

Brian S. Leander, Departments of Botany and Zoology, University of British Columbia, #3529-6270 University Blvd., Vancouver, BC, V6T 1Z4, Canada. E-mail: bleander@interchange.ubc.ca

Introduction

Gregarines are single-celled parasites of the intestinal lumena and coelomic cavities of invertebrates, especially polychaetes and insects. These parasites comprise a large group of apicomplexans with diverse cell morphologies and modes of locomotion (Grassé 1953; Levine 1971, 1976, 1977a, 1977b; Leander *et al*. 2003b; Leander 2006). Because of their widespread presence in animals and a long history of being overlooked by the scientific community, it is expected that the vast majority of gregarines remains unknown. Both ultrastructural and molecular data suggest that certain gregarines, so-called 'archigregarines', display morphostasis and possess several characteristics that have been retained from the most recent common ancestor of all apicomplexans (Grassé 1953; Cox 1994; Leander & Keeling 2003). For instance, the lifecycle of archigregarines is completed in marine environments within the intestinal lumen of a single invertebrate host. Moreover, some archigregarines possess: (1) extracellular

'trophozoites' (feeding stages) that putatively use a myzocytosis-based mode of feeding and otherwise resemble the infective 'sporozoites' of most other apicomplexans; and (2) oocysts that contain only four infective sporozoites (Grassé 1953; Schrével 1971b; Théodoridès 1984; Schrével & Philippe 1993; Cox 1994; Leander & Keeling 2003; Leander *et al*. 2003b, 2006). This combination of characteristics is reminiscent of the nearest free-living relatives to the strictly parasitic Apicomplexa, namely a group of predatory biflagellates called 'colpodellids' (Kuvardina *et al*. 2002; Leander & Keeling 2003; Leander *et al*. 2003c; Cavalier-Smith & Chao 2004). Accordingly, broad molecular phylogenetic data coupled with comparative ultrastructural information from archigregarines is fundamental for inferring the early evolutionary history of the Apicomplexa as a whole and gregarines in particular.

Archigregarines are perhaps best represented by the genus *Selenidium* (Ray 1930; MacKinnin & Ray 1933; Vivier & Schrével 1964, 1966; MacGregor & Thomas 1965; Schrével 1968, 1970, 1971a, 1971b; Levine 1971; Stebbings *et al*. 1974; Mellor & Stebbings 1980; Kuvardina & Simdyanov 2002; Leander *et al*. 2003b, 2006). The trophozoites are generally vermiform or spindle-shaped and develop from smaller spindle-shaped sporozoites that are attached to host epithelial cells. The wide range of cell sizes within a single population of trophozoites reflects this maturation process. Regardless of size, the trophozoites of *Selenidium* tend to be highly motile and are capable of bending and coiling, especially when dislodged from host tissues. The surface of *Selenidium* trophozoites is reinforced with a well-developed system of microtubules and is usually inscribed with several parallel grooves orientated longitudinally; the grooves define 4–50 broad pellicular folds, depending on the species (Ray 1930; Vivier & Schrével 1964; Levine 1971; Schrével 1971b; Leander *et al*. 2003b). The larger trophozoites eventually pair up in a process called 'syzygy', which marks the onset of gamete formation and sexual reproduction. In some species of archigregarines, the sporozoites are thought to replicate asexually in a process known as 'schizogony' (syn. merogony). Schizogony is not necessarily apparent in every sample and therefore is difficult to demonstrate. Accordingly, I have not adopted the proposed taxonomic scheme, based on the presumed absence of schizogony in some species, that splits *Selenidium* species with nearly identical trophozoite morphologies into two different genera, each within different orders: *Selenidioides* within Archigregarinorida (schizogony observed) and *Selenidium* within Eugregarinorida (schizogony not observed) (Levine 1971). In concurrence with other authors (Schrével 1971a, 1971b; Gunderson & Small 1986; Kuvardina & Simdyanov 2002; Leander *et al*. 2003b), I define archigregarines based on the trophozoite morphology (and behaviour) described above and treat *Selenidioides* as a junior synonym of *Selenidium*. Nonetheless, *Selenidium* is a diverse and taxonomically problematic genus (MacKinnin & Ray 1933; Levine 1971), and it remains to be determined — with both ultrastructural and molecular data — how closely related the species within this taxon actually are.

Molecular phylogenetic data from gregarines, especially archigregarines, is scanty, mainly because gregarines have never been cultured and must be manually isolated from hosts collected in the field. Although some protein genes have been successfully amplified from a few terrestrial gregarines, namely *Monocystis* and *Gregarina* (Leander *et al*. 2003a; Heintzelman 2004; Leander & Keeling 2004; Omoto *et al*. 2004), most molecular phylogenetic studies of gregarines have focused on sequences of the small subunit ribosomal RNA gene (SSU rDNA) (Carreno *et al*. 1999; Leander *et al*. 2003a, 2003b, 2006). Among the most significant outcomes of this work so far is the possible sister relationship between gregarines and *Cryptosporidium* (Carreno *et al*. 1999; Leander *et al*. 2003a, 2003b; Leander & Keeling 2004). *Cryptosporidium* species infect the intestinal systems of vertebrates, including humans, and are currently classified with other parasites of vertebrates in a different group of apicomplexans altogether, namely eimeriid coccidians (Zhu *et al*. 2000; Beyer *et al*. 2002; Deng *et al*. 2004). If *Cryptosporidium* is truly more closely related to gregarines than to coccidians, then *Cryptosporidium* biology would need to be interpreted in a brand new light. However, this light must be powered by knowledge of gregarines, which is currently severely lacking. Because both *Cryptosporidium* and gregarines tend to branch early in apicomplexan molecular phylogenies, the addition of sequences from diverse archigregarines (e.g., *Selenidium* species) is expected to help refine and further resolve the phylogenetic position of *Cryptosporidium*.

The emerging molecular phylogenetic framework has also demonstrated that substitution rates in gregarine SSU rDNA and some protein genes (e.g., β-tubulin) are exceptionally high (Leander *et al*. 2003a, 2006; Leander & Keeling 2004). The shortest known gregarine branch in SSU rDNA phylogenies comes from an archigregarine, namely *Selenidium terebellae*, which might reflect stasis in this lineage not only at the morphological level, as discussed previously, but also at the molecular level. Nonetheless, as the taxon sample for gregarines has increased, so has the internal resolution of gregarine relationships, resulting in several well supported subclades (e.g., lecudinid eugregarines, monocystid eugregarines, septate eugregarines and neogregarines). Moreover, the addition of SSU rDNA sequences from known gregarines has significantly bolstered the number of reference taxa needed to interpret the cellular origins of unknown sequences derived from environmental PCR surveys (Dawson & Pace 2002; Moreira & Lopez-Garcia 2003; Leander *et al*. 2003a, 2003c; Berney *et al*. 2004; Cavalier-Smith 2004).

These preliminary insights have demonstrated that interpretations of PCR surveys, especially of marine environments, will become considerably more refined as knowledge of gregarines advances. To this end, I have characterised the ultrastructural properties and the molecular phylogenetic position of *S. serpulae*, an intestinal archigregarine parasite of the calcareous tubeworm *Serpula vermicularis*.

Materials and methods

Collection of organisms

Ten individuals of the calcareous tubeworm *Se. vermicularis* Linnaeus were collected at low tide (0.2–0.3 m above the mean low tide) from the rocky pools of Grappler Inlet near the Bamfield Marine Sciences Centre, Vancouver Island, Canada in June 2004. Trophozoites that conformed to the species description of *S. serpulae* (Lankester) Caullery and Mesnil 1899 were isolated from the intestines of five different worms.

Light microscopy

Trophozoites were observed and micromanipulated with a Leica MZ6 stereomicroscope and a Leica DMIL inverted microscope; integrated modulation contrast (IMC) images were captured using a PixeLink Megapixel colour camera attached to the Leica DMIL inverted microscope. Micropipetted trophozoites were washed with filtered seawater and placed on a glass specimen slide. Digital movies (12 frames/s) and DIC images of individual trophozoites were produced with a Zeiss Axiovert inverted microscope connected to the PixeLink Megapixel colour camera.

Scanning electron microscopy

Trophozoites were released into seawater by teasing apart the intestine of the tubeworms with fine-tipped forceps. Approximately 20 parasites were removed from the remaining gut material by micromanipulation and washed twice in filtered seawater. Individual trophozoites were deposited directly into the threaded hole of a Swinnex filter holder, containing a 5 μm polycarbonate membrane filter (Coring Separations Division, Acton, Massachusetts) submerged in 10 mL of seawater within a small canister (2 cm dia. and 3.5 cm tall). Whatman filter paper was mounted on the inside base of a beaker (4 cm dia. and 5 cm tall) and saturated with 4% OsO_4. Placing the beaker over the canister fixed the parasites with OsO_4 vapours. After 30 min of vapour fixation, six drops of 4% OsO_4 were added directly to the seawater and the parasites were fixed for an additional 30 min. A 10 mL syringe filled with 30% ethanol was screwed to the Swinnex filter holder and the entire apparatus was removed from the canister containing seawater and fixative. The trophozoites were dehydrated with a graded series of ethyl alcohol and critical point dried with CO_2. Filters were mounted on stubs, sputter coated with gold, and viewed under a Hitachi S4700 Scanning Electron Microscope. Some SEM micrographs were created from montages of three individual images of the same cell and illustrated on black backgrounds using Adobe Photoshop 6.0 (Adobe Systems, San Jose, CA).

Transmission electron microscopy

Dissected pieces of trophozoite-infected intestines (approximately 5 mm long) were deposited into a 1.5 mL Eppendorf tube and prefixed with 2% (v/v) glutaraldehyde in unbuffered seawater at 4 °C for 60 min. The intestinal pieces were washed twice in unbuffered seawater before post-fixation in 1% (w/v) OsO_4 for 60 min at room temperature. The intestinal pieces were dehydrated through a graded series of ethanol, infiltrated with acetone–resin mixtures (pure acetone, 3 : 1, 1 : 1, 1 : 3, pure Epon 812 resin) and flat-embedded in Epon 812 resin on a microscope slide. Following polymerised at 60 °C, the intestinal pieces were manually excised with a razor blade, mounted on blank blocks using superglue and sectioned with a diamond knife on a Leica Ultracut Ultra-Microtome. Thin sections (70–80 nm) were post-stained with uranyl acetate and lead citrate and viewed under a Hitachi H7600 Transmission Electron Microscope.

DNA isolation, PCR, cloning and sequencing

One hundred and fifty trophozoites were manually isolated from dissected hosts, washed three times in filtered seawater and deposited into 1.5 mL Eppendorf tubes. DNA was extracted with a standard CTAB extraction protocol: pelleted parasites were suspended in 200 μL CTAB extraction buffer (1.12 g Tris, 8.18 g NaCl, 0.74 g EDTA, 2 g CTAB, 2 g polyvinylpyrolidone, 0.2 mL 2-mercaptoethanol in 100 mL water), incubated at 65 °C for 30 min and separated with chloroform:isoamyl alcohol (24 : 1). The aqueous phase was then precipitated in 70% ethanol.

The SSU rRNA gene from *S. serpulae* was amplified as a single fragment using PCR primers described previously (Leander *et al.* 2003a). PCR products corresponding to the expected size were gel isolated and cloned into the pCR 2.1 vector using the TOPO TA cloning kit (Invitrogen, Frederick, MD, USA). Eight cloned plasmids were digested with *EcoR1* and screened for size. Two clones were sequenced with ABI big-dye reaction mix using vector primers orientated in both directions. The SSU rDNA sequence was identified by BLAST analysis and deposited in GenBank (Accession number DQ683562).

Molecular phylogenetic analysis

The new sequence from *S. serpulae* was aligned with 51 other alveolate SSU rDNA sequences using MacClade 4 (D. R. Maddison & W. P. Maddison 2000) and visual fine-tuning. The apicomplexan sequence misattributed to the foraminiferan

Ammonia beccarii (U07937) was omitted from the analyses because this sequence is missing data (Wray *et al*. 1995; Leander *et al*. 2003a, 2003b). A 54-taxon alignment was also constructed by the addition of two short sequences derived from an environmental PCR survey of a hydrothermal vent system, namely C1-E017 (AY046619) and C2-E016 (AY046806). Maximum likelihood (ML), distance and Bayesian methods under different DNA substitution models were performed on the 52-taxon alignment and the 54-taxon alignment, each containing 1159 and 803 unambiguously aligned sites, respectively; all gaps were excluded from the alignments prior to phylogenetic analysis. The alpha shape parameters were estimated from the 52-taxon dataset using HKY and a gamma distribution with invariable sites and eight rate categories (alpha = 0.47; Ti/Tv = 1.85; fraction of invariable sites = 0.09). Gamma-corrected ML trees (analysed using the alpha shape parameter listed above) were constructed with PAUP* 4.0 using the general time reversible (GTR) model for base substitutions (Posada & Crandall 1998; Swofford 1999). Gamma corrected ML tree topologies found with HKY and GTR were identical. ML bootstrap analyses were performed in PAUP* 4.0 (Swofford 1999) on 100 re-sampled datasets under an HKY model using the alpha shape parameter and transition/transversion ratio (Ti/Tv) estimated from the original dataset.

Distances for the SSU rDNA datasets were calculated with TREE-PUZZLE 5.0 using the HKY substitution matrix (Strimmer & Von Haeseler 1996) and trees were constructed with weighted neighbor-joining (WNJ) using WEIGHBOR (Bruno *et al*. 2000). Five hundred bootstrap datasets were generated with SEQBOOT (Felsenstein 1993). Respective distances were calculated with the shell script 'puzzleboot' (M. Holder and A. Roger, www.tree-puzzle.de) using the alpha shape parameter and transition/transversion ratios estimated from the original dataset and analysed with Weighbor.

We also examined the SSU rDNA datasets with Bayesian analysis using the program MRBAYES 3.0 (Huelsenbeck & Ronquist 2001). The program was set to operate with GTR, a gamma distribution and four Monte-Carlo-Markov chains (MCMC) (default temperature = 0.2). A total of 2 000 000 generations were calculated with trees sampled every 100 generations and with a prior burn-in of 200 000 generations (2000 sampled trees were discarded). A majority rule consensus tree was constructed from 16 000 post-burn-in trees with PAUP* 4.0. Posterior probabilities correspond to the frequency at which a given node is found in the post-burn-in trees.

GenBank accession numbers

(AF494059) *Adelina bambarooniae* (AF274250) *Amphidinium asymmetricum* (AY603402) *Babesia bigemina* (DQ273988) *Rhytidocystis polygordiae* (M97909) *Blepharisma americanum* (M97908) *Colpoda inflata* (AY078092) *Colpodella pontica* (AF330214) *Colpodella tetrahymenae* (M64245) *Crypthecodinium cohnii* (L19068) *Cryptosporidium baileyi* (AF093489) *Cryptosporidium parvum* (AF093502) *Cryptosporidium serpentis* (AF39993) *Cytauxzoon felis* (U67121) *Eimeria tenella* (AY179975, AY179976, AY179977, AY179988, AY046619, AY046806) Environmental sequences (AF022155) *Gonyaulax spinifera* (AF129882) *Gregarina niphandrodes* (AJ415513) *Gymnodinium sanguineum* (AF274261) *Gyrodinium dorsum* (AF286023) *Hematodinium* sp. (AF130361) *Hepatozoon catesbianae* (AF274268) *Kryptoperidinium foliaceum* (DQ093796) *Lankesteria abbotti* (AF080611) *Lankesterella minima* (AY196706) *Lecudina polymorpha* morphotype 1 (AF457128) *Lecudina tuzetae* (AF457130) *Leidyana migrator* (AF521100) *Lessardia elongata* (DQ093795) *Lithocystis* sp. (AB000912) Marine parasite from *Tridacna crocea* (AY334568) *Mattesia geminata* (AF457127) *Monocystis agilis* (AJ271354) *Neospora caninum* (AF022200) *Noctiluca scintillans* (AF129883) *Ophryocystis elektroscirrha* (M14601) *Oxytricha nova* (X03772) *Paramecium tetraurelia* (AF126013) *Perkinsus marinus* (AY033488) *Pfiesteria piscicida* (Y16233) *Prorocentrum panamensis* (DQ093794) *Pterospora floridiensis* (DQ093793) *Pterospora schizosoma* (M64244) *Sarcocystis muris* (AF274276) *Scrippsiella sweeneyae* (DQ683562) *Selenidium serpulae* (AY196709) *Selenidium terebellae* (AY196708) *Selenidium vivax* (AF013418) *Theileria parva* (M97703) *Toxoplasma gondii*.

Results

Cell surface, cytoskeleton and motility

Relaxed trophozoites took the form of elongated spindles and varied considerably in size, ranging from 70 to 190 μm long by 7–25 μm wide (n = 30) (Fig. 1A–D). The broad range of cell sizes presumably reflected different stages in development from smaller sporozoites. The anterior end of trophozoites could be recognised by the slightly anterior position of the otherwise centrally positioned nucleus and by distinctive bending movements associated with a relatively slender neck situated behind a nipple-shaped anterior protuberance (Fig. 1A,B,L). Moreover, once trophozoites were dislodged from the host intestinal epithelium, the anterior end gradually began to swell forming a dome-shaped end (Fig. 1C,D). Trophozoites were capable of bending, twisting and contracting their cell shape, movements that are perhaps best described as nematode-like (Fig. 1F–M). The dislodged trophozoites also rotated continuously and slowly around their longitudinal axis.

The trophozoite surface was sulcated with about 6–9 broad longitudinal folds per side (Figs 1B and 2A); transverse TEMs demonstrated the presence of between 19 and 23 folds around the entire cell (Fig. 2D). The longitudinal folds on the convex surfaces of bent trophozoites were wider and shallower than the folds on the concave surfaces (Fig. 2B,D). The crests of the longitudinal folds forming the concave surfaces of contracted trophozoites were covered with a dense array of parallel transverse folds (Fig. 2B,C).

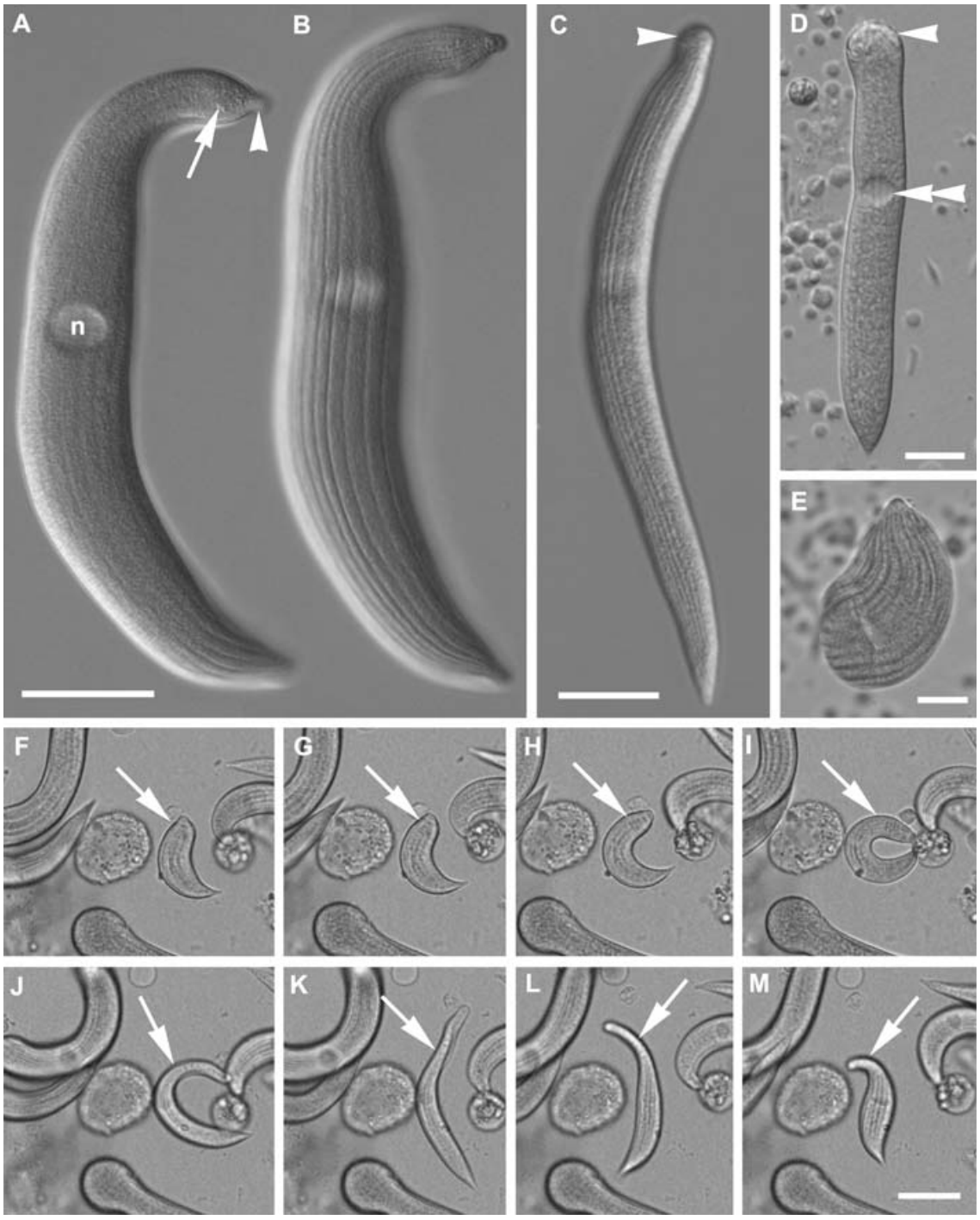

Fig. 1 A–M. Light micrographs of the trophozoites of *Selenidium serpulae* isolated from the intestines of the calcareous tubeworm, *Serpula vermicularis*. —A, B. Differential interference contrast (DIC) micrographs showing the centrally positioned nucleus (n), granular material (arrow) located behind an anterior nipple (arrowhead) and the sulcated surface consisting of longitudinal folds (Bar = 15 μm). —C. Integrated modulation contrast (IMC) micrograph showing a slender trophozoite with an anterior tip that is beginning to swell (arrowhead) (Bar = 20 μm). —D. IMC micrograph showing a trophozoite with a centrally positioned nucleus (double arrowhead) and a severely swollen anterior tip (arrowhead) (Bar = 10 μm). —E. IMC micrograph showing a contracted trophozoite with the anterior tip orientated upward (Bar = 5 μm). —F–M. A time series of IMC micrographs (1 frame/s) showing the general cell shapes and bending movements of a trophozoite (arrows); the anterior end of the cell is orientated upward (Bar = 20 μm).

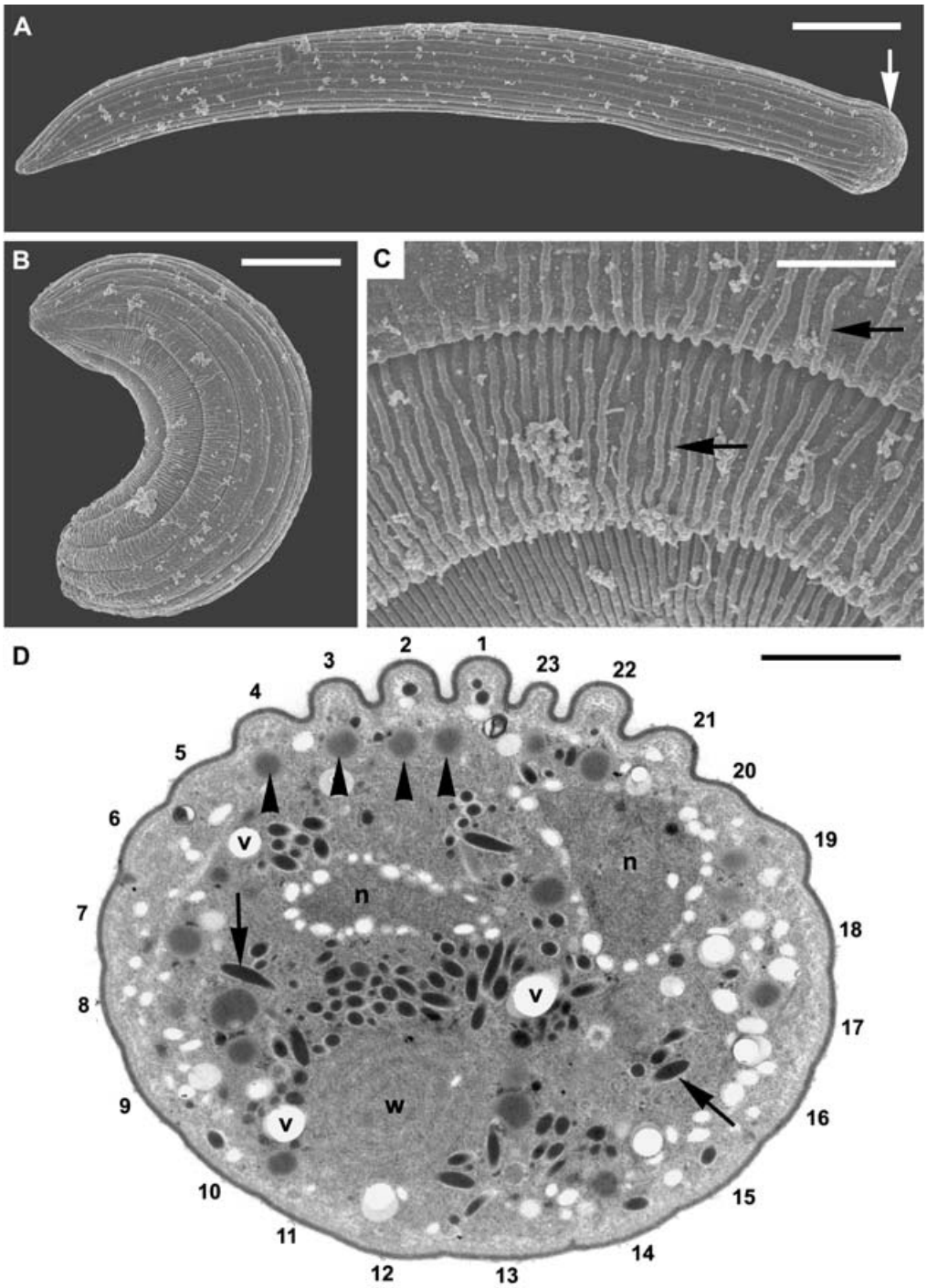

Fig. 2 A–D. Scanning and transmission electron micrographs (SEM and TEM) of the trophozoites of *Selenidium serpulae*. —A. SEM of an extended trophozoite showing the longitudinal folds and a swollen anterior tip (arrow) (Bar = 15 μm). —B. Low magnification SEM of a contracted trophozoite showing textural differences on the convex and concave surfaces (Bar = 10 μm). —C. High magnification SEM of a contracted trophozoite showing the organization of transverse folds (arrows) on the concave surface (Bar = 10 μm). —D. Transverse TEM showing the general ultrastructure of trophozoites. This section demonstrates 23 longitudinal surface folds, and the elevated surface folds (folds 21, 22, 23, 1, 2, 3 and 4) indicate that the concave surface of the bent trophozoite is orientated upward. The section also shows dense bodies (arrows), vesicles (v), lipid droplets (arrowheads), two nuclear profiles of a lobular nucleus (n), and a region containing a faint whorled pattern of unknown homology (w). Mitochondria were not observed (Bar = 2 μm).

The trilayered inner membrane complex, consisting of the plasma membrane and two alveolar membranes, was robust and reinforced by a single layer of subtending microtubules (Fig. 3B,C). The continuity of this microtubular layer was interrupted across the bottom of the pellicle grooves (Fig. 3B). Each microtubule was encased within an electron transparent sheath that took on a square or hexagonal shape in transverse view (Fig. 3B,C). Clusters of loosely arranged microtubules occupied deeper positions within the cytoplasm of the folds and were also surrounded by electron transparent sheaths (Fig. 3B). Tangential sections through the folds demonstrated that some of the deep microtubules were orientated obliquely relative to the longitudinal axis of the trophozoites (Fig. 3D).

Organelles, micropores and pinocytotic vesicles

The centrally positioned nucleus was spherical or lobular in shape and about 4 μm in diameter (Figs 3A and 4B). Two nuclear profiles in some micrographs are inferred to be the result of transverse sections through the periphery of a lobular nucleus (Fig. 2D). The nuclei contained a conspicuous nucleolus pressed against the nuclear envelope (Figs 3A and 4A) and, in one instance, an internal vacuole that was approximately the same size as the nucleolus (Fig. 4A). A coat of closely spaced vesicles surrounded the nuclear envelope (Figs 2D, 3A and 4B).

Carbohydrate storage products in the form of amylopectin were not definitively observed in the trophozoites. Putative mitochondria were observed, but they were inconspicuous and apparently highly reduced (Fig. 4B, inset). The cytoplasm contained several other structures known from other gregarines, such as lipid droplets about 0.3–0.5 μm in diameter, rod-shaped dense bodies, Golgi bodies, large vesicles, ribosome-studded cisternae of endoplasmic reticulum, and a structure consisting of a dense accumulation of concentric membranes (Figs 2D, 3A and 4B,F,G). Moreover, micropores were present in the bottom of the grooves between surface folds (Fig. 4B,C). The micropores gave rise to multiple membrane-bound pinocytotic vesicles (syn. lipochondria) that were often connected to the inner membrane complex by a peduncle (Figs 3B and 4D). When viewed in transverse section, the peduncles consisted of two parallel membranes orientated perpendicularly to the longitudinal axis of the surface folds (Fig. 5F). The pinocytotic vesicles were about 0.3 μm in diameter and contained 2–6 concentric membranes (Fig. 4E). The cytoplasm also contained an inconspicuous whorled structure with unknown homology in other known gregarines (Fig. 2D).

Attachment apparatus

Trophozoites occupied the intestinal lumen of the host and were attached to the ciliated epithelium by the anterior end or mucron (Fig. 5A). When attached, the cells were tranquil and postured in the form of a curved spindle with the concave surface facing toward the ciliated epithelium (Fig. 5A). The anterior end of the trophozoite was embedded within a single host epithelial cell approximately 5 μm deep, but was completely engulfed by the cilia of adjacent epithelial cells (Fig. 5A–E). Remnant debris of the host epithelial cells remained fixed to the anterior tip of dislodged trophozoites (Fig. 5D). Although a distinct conoid or polar ring was not observed, a dense array of parallel microtubules emanated from a densely stained layer at the anterior tip of the trophozoites (Fig. 5F). A search for the presence of a conoid was not comprehensive and is the subject of a future study. Nonetheless, necrosis of the host epithelial cells was evident in the trophozoite attachment zone (Fig. 5E,F).

Molecular phylogeny as inferred from SSU rDNA

Phylogenetic analyses of the 52-taxon dataset showed a strongly supported clade of ciliate sequences and a poorly resolved backbone relating dinoflagellates + *Perkinsus*, colpodellids and several different clades of apicomplexans (Fig. 6). The sequences from intestinal gregarine apicomplexans were particularly divergent and formed a weakly supported clade consisting of archigregarines, septate eugregarines and marine aseptate eugregarines (Fig. 6). The sister clade to the intestinal gregarines consisted of two environmental sequences of unknown cellular identity, namely AY179975 and AY179976. The three *Selenidium* species represented the archigregarines and paraphyletically diverged at the origin of the intestinal gregarine clade; *S. terebellae* diverged first, followed be a modestly supported clade consisting of *S. vivax* and *S. serpulae* (Fig. 6). The septate eugregarines (*Gregarina* and *Leidyana*) from terrestrial insects formed a strongly support sister clade to a clade consisting of all of the marine aseptate eugregarines in the dataset, namely *Lecudina*, *Pterospora*, *Lithocystis* and *Lankesteria*. The terrestrial monocystid eugregarines and neogregarines, together, formed a strongly supported clade that did not show any clear affinity to the intestinal gregarines. Moreover, the poorly resolved apicomplexan backbone gave rise to other clades with indeterminable sister groups, namely rhytidocystids, cryptosporidians and a modestly supported clade consisting of adeleorinans, eimeriids and piroplasmids (Fig. 6).

The top two BLAST hits for the new sequence from *S. serpulae* were short sequences derived from a environmental PCR survey near a hydrothermal vent in the Gulf of California, namely C1-E017 (AY046619) and C2-E016 (AY046806). Because the two additional environmental sequences were only 1088 bp in length, they were not included in the 52-taxon dataset. Accordingly, a 54-taxon dataset containing all of the sequences in the 52-taxon dataset plus the two environmental sequences (803 unambiguously aligned sites) was analysed

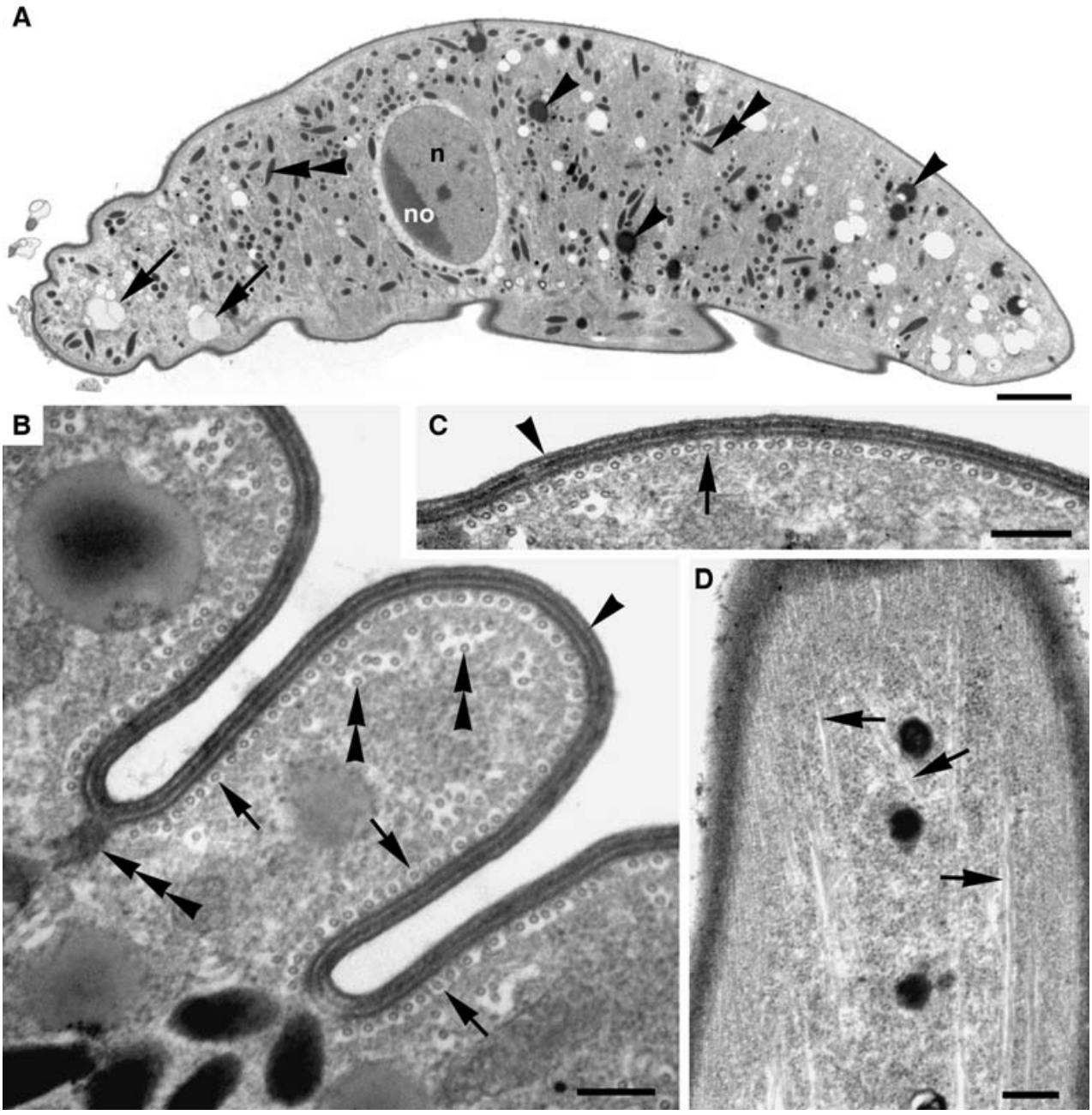

Fig. 3 A–D. Transmission electron micrographs (TEM) of the trophozoites of *Selenidium serpulae*. —A. Longitudinal TEM showing the centrally positioned nucleus (n), prominent nucleolus (no), vesicles (arrows), dense bodies (double arrowheads) and lipoprotein droplets (arrowheads). The anterior end is orientated to the left (Bar = 2 μm). —B, C. Transverse TEMs through the trophozoite surface showing three longitudinal surface folds, the trilayered inner membrane complex (arrowhead) and a single row of subtending microtubules, each surrounded by an electron transparent sheath (arrows). Several loosely organized microtubules (double arrowheads) were also found deeper within the cytoplasm of the folds. A peduncle-like structure (triple arrowhead) branched into the cytoplasm from the bottom of one groove (Bars = 0.2 μm). —D. Tangential TEM through a longitudinal surface fold showing that the deeper microtubules (arrows) often have oblique orientations relative to the longitudinal axis of the cell (Bar = 0.25 μm).

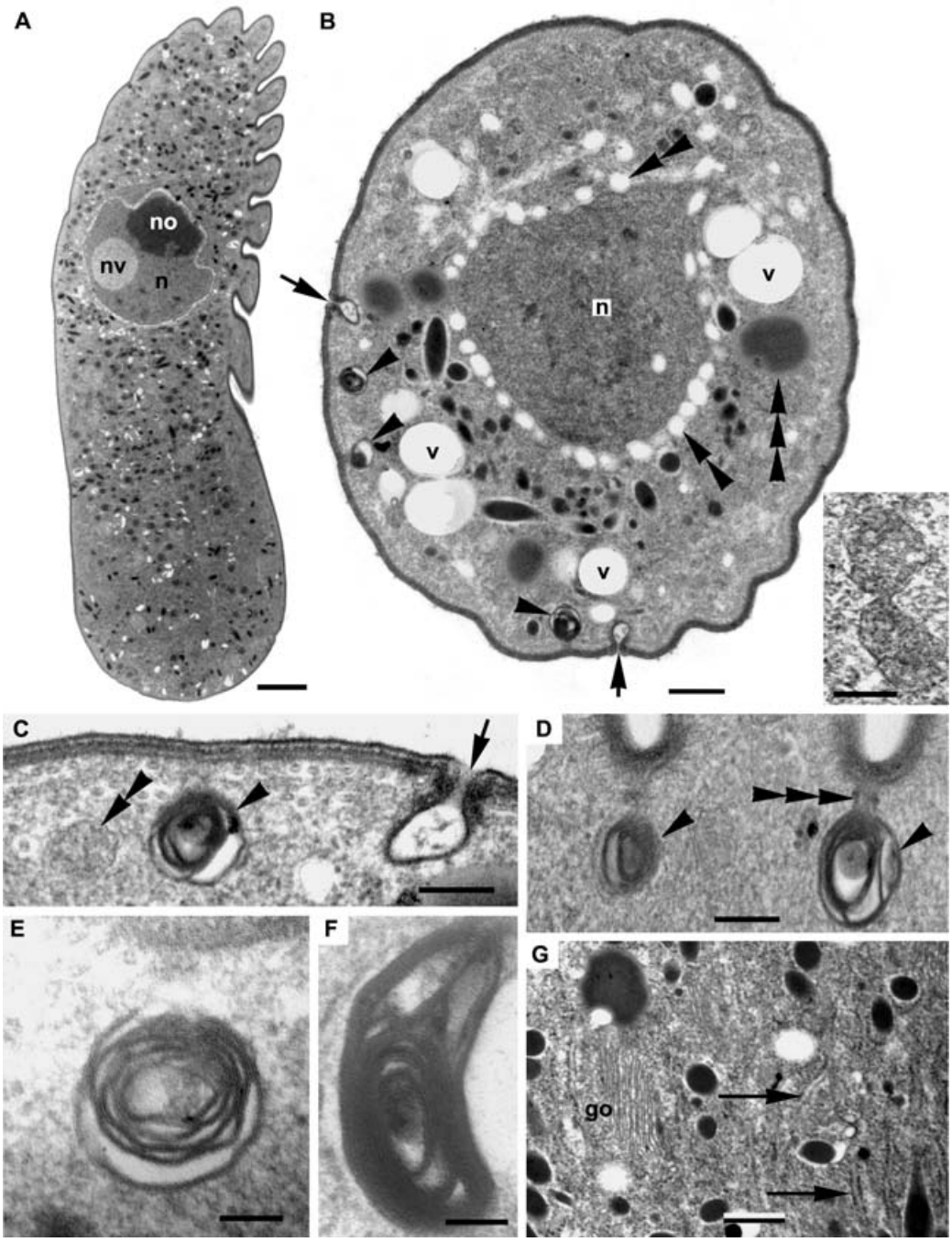

Fig. 4 A–G. Transmission electron micrographs (TEM) of the trophozoites of *Selenidium serpulae*. —A. Oblique TEM through a trophozoite showing the lobular shape of the nucleus (n) containing a prominent nucleolus (no) and a nuclear vacuole (nv) (Bar = 2 μm). —B. Transverse TEM through a trophozoite showing a large nuclear profile (n), a peripheral coat of nuclear vesicles (double arrowheads), lipoprotein droplets (triple arrowheads), large vesicles (v), micropores (arrows) and multiple membrane-bound pinocytotic vesicles (syn. lipochondria) positioned beneath the grooves between surface folds (arrowheads) (Bar = 0.5 μm). Inset: A high magnification TEM showing a putative, but inconspicuous, mitochondrion (Bar = 0.1 μm). —C, D. High magnification TEMs showing a putative mitochondrion (double arrowhead), micropores (arrow) and multiple membrane-bound pinocytotic vesicles (arrowheads) connected to the bottom of the grooves by a peduncle (triple arrowheads) (Bars = 0.2 μm). —E. High magnification TEM of a pinocytotic vesicle (Bar = 0.1 μm). —F. High magnification TEM showing an unidentified structure consisting of a dense accumulation of concentric membranes (Bar = 0.1 μm). —G. TEM showing a typical Golgi body (go) and ribosome-studded cisternae of endoplasmic reticulum (arrows) (Bar = 0.5 μm).

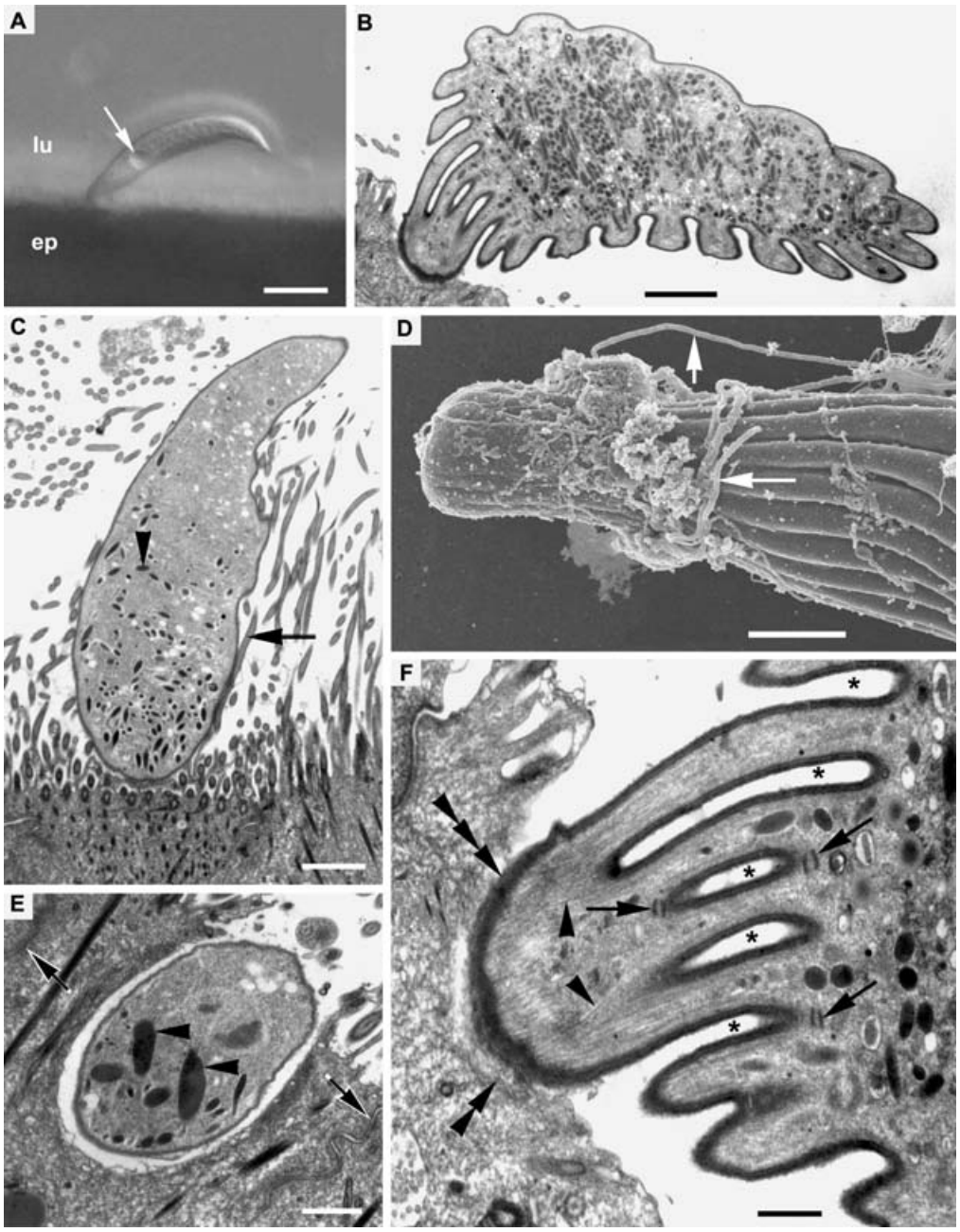

Fig. 5 A–F. The attachment apparatus of the trophozoites of *Selenidium serpulae*. —A. Light micrograph showing a trophozoite suspended in the intestinal lumen of its host (lu) while attached to the ciliated epithelium (ep). The anterior end of the spindle shaped trophozoites can be recognised by the slightly anterior position of the nucleus (arrow) (Bar = 30 μm). —B, C. Oblique transmission electron micrographs (TEM) through the anterior end of attached trophozoites showing the abundance of dense bodies within the cytoplasm and neighbouring cilia (arrow) stemming from the host's epithelial cells (Bars = 2 μm). —D. Scanning electron micrograph of the anterior tip of a dislodged trophozoite showing remnants of the host cilia (arrows) and, presumably, other cellular debris derived from the host epithelium (Bars = 2 μm). —E. Oblique TEM through the anterior tip of a trophozoite that is embedded within a host epithelial cell; cell–cell junctions between adjacent epithelial cells are also shown (arrows). Dense bodies are shown (arrowheads), but no evidence of a conoid was observed (Bars = 1 μm). —F. Tangential TEM through the anterior tip of a trophozoite showing an array of parallel microtubules (arrowheads) stemming from an electron-dense layer (triple arrowhead) that is probably a micotubule organizing centre (MTOC). Evidence of host cell necrosis (double arrowhead) is present just outside of this dense layer. The TEM also shows the transverse ultrastructure of the peduncles (arrows) leading to the multiple membrane-bound, pinocytotic organelles. The peduncles consist of two parallel membranes and are positioned beneath the surface grooves (asterisks) (Bars = 0.5 μm).

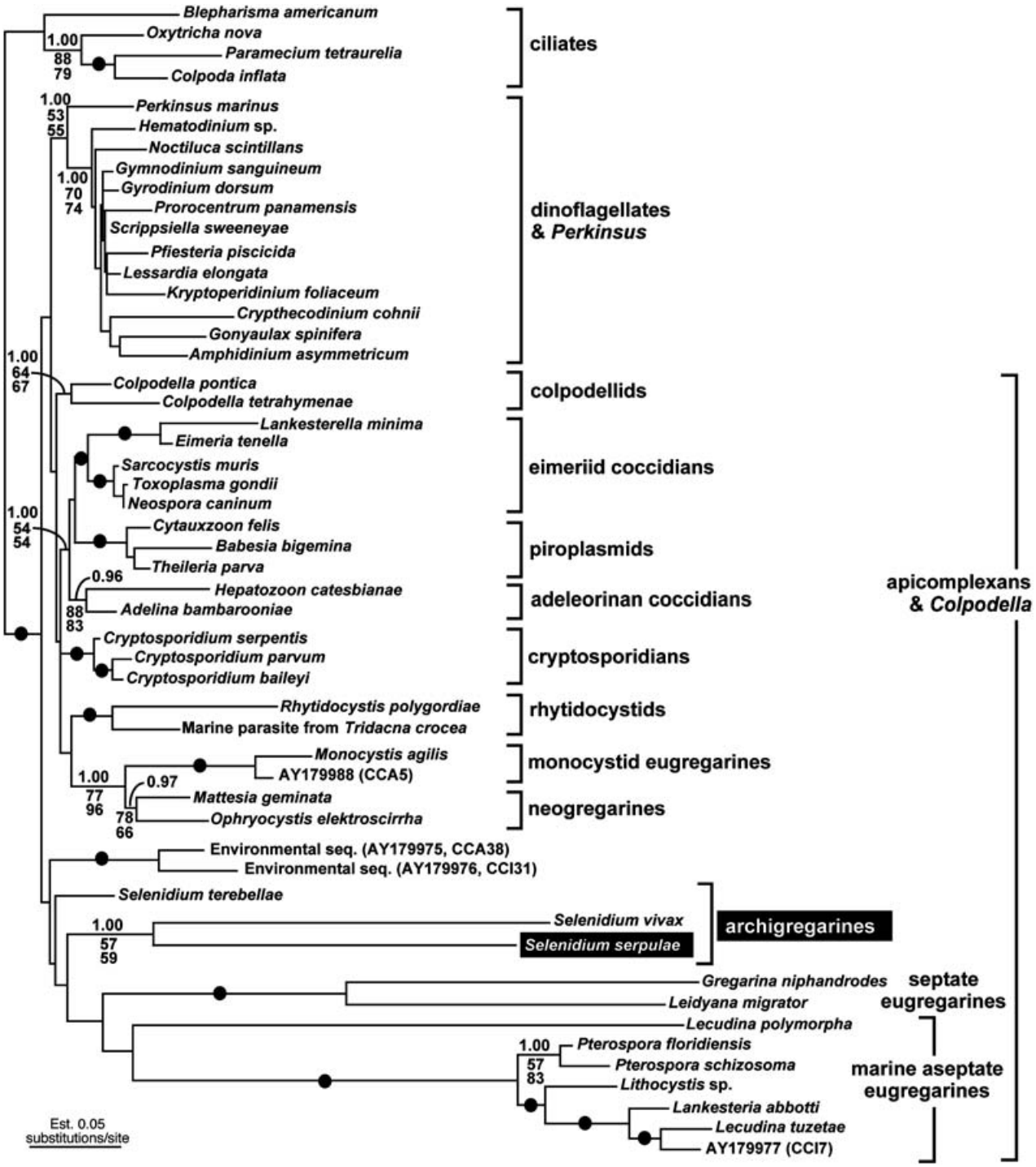

Fig. 6 Gamma-corrected maximum likelihood tree (–ln L = 14526.312, $\alpha = 0.47$, eight rate categories) inferred using the GTR model of substitution on an alignment of 52 SSU rDNA sequences and 1165 unambiguously aligned sites. Numbers at the branches denote Bayesian posterior probabilities — GTR (top), bootstrap percentages using maximum likelihood — HKY (middle) and bootstrap percentages using weighted neighbor-joining (bottom). Black dots on branches denote posterior probabilities and bootstrap percentages of 90% or higher. The sequence derived from this study is highlighted in the shaded box.

separately (data not shown). These phylogenetic analyses supported the BLAST results and produced a robust clade consisting of *S. serpulae* and the two hydrothermal vent sequences (Bayesian posterior probability = 1.0; ML boostrap = 100; Weighbor bootstrap = 100). The distant sister lineage to the *S. serpulae* clade was *S. vivax*; bootstrap and Bayesian support for this relationship was consistent with the results derived from the 52-taxon dataset (Fig. 6).

Discussion

Comparative and functional morphology

A 'standard' apical complex was not observed in the trophozoites of *S. serpulae*. Densely stained bodies were distributed throughout the cytoplasm, but none were distinguishable as rhoptries. Although a conoid was not observed in this study, whether this feature was simply unnoticed with the TEM cannot be ruled out, and seems likely. A search for the presence of a conoid was not comprehensive and is the subject of a future study. Nonetheless, the thick electron-dense layer at the anterior tip of the trophozoites in *S. serpulae* is probably a microtubule-organizing centre (MTOC) from which the longitudinally arranged subpellicular microtubules emanate. A similar structure has been described from another archigregarine parasite, namely *Digyalum oweni* of littorinid gastropods (Dyson *et al*. 1993). However, once the mucron of *S. serpulae* was dislodged from the host epithelium, it gradually became a dome-shaped swelling. This suggests that the structural integrity of the nipple-shaped mucron, in the absence of the scaffolding provided by a conoid, is dependent on being attached to the epithelial cells of the host. To my knowledge, swollen anterior ends have only been observed in the trophozoites of eugregarines (which also lack a conoid) and one other archigregarine, namely *S. cometomorpha* (Schrével 1970).

The known morphological diversity and the emerging molecular phylogenetic framework for gregarines indicate that the number of longitudinal folds on the surface of trophozoites has increased over time (Levine 1971, 1976, 1977b; Leander *et al*. 2003b, 2006). This evolutionary transformation of the cell surface corresponds with shifts in nutritional mode and locomotion (Leander *et al*. 2006). Many archigregarines, for instance, have retained the apical complex in the trophozoite stages and appear to employ a myzocytosis-based mode of nutrition (i.e., the ability to pierce a host cell and withdraw its contents into a phagocytic vesicle) along with surface-mediated nutrition via pinocytosis. The trophozoites of archigregarines possess only a few epicytic folds, ranging from 4 to about 50, and undergo active bending and coiling movements. Moreover, the trilayered inner-membrane complex is robust and subtended by linear rows of longitudinal microtubules, each surrounded by an electron transparent sheath (syn. sleeve) (Vivier & Schrével 1964; Schrével 1971a; Stebbings *et al*. 1974). The function of the microtubular sheaths remains to be determined, but they are assumed to play an important role in microtubular sliding, which was demonstrated by completely immobilising the trophozoites of *S. fallax* following exposure to colchicine (Stebbings *et al*. 1974; Mellor & Stebbings 1980). Some archigregarines possess a single, continuous row of microtubules beneath the pellicle folds, as in *S. serpulae*, whereas others have two or three rows (e.g., *Selenidium* sp. from *Sabellaria alveolata*) (Vivier & Schrével 1964). Regardless, the rows of microtubules invariably contain discontinuities beneath the pellicle grooves, which facilitate pinocytosis.

Previous authors have proposed that the most dynamic trophozoites are correlated with more developed microtubular systems, and that the distinctive movements of archigregarines are reminiscent of the whiplash undulations employed by nematodes (Schrével 1971a; Stebbings *et al*. 1974; Mellor & Stebbings 1980). Nematodes lack circular muscle and are restricted to a superficial arrangement of longitudinal muscles (and obliquely orientated 'muscle arms') that function antagonistically against a robust but elastic cuticle. Moreover, some nematodes also have sulcated bodies that resemble the folded pellicle of *S. serpulae* and other archigregarines. Therefore, the best hypothetical framework for understanding the mechanism behind archigregarine motility is that the inner-membrane complex and longitudinal microtubules together represent a unicellular analogue to the musculocuticular system of nematodes (Stebbings *et al*. 1974). The functional significance of the bending and coiling movements of archigregarines presumably enables the trophozoites to find syzygy partners, infect adjacent epithelial cells and move nutrients across their cell surfaces within the intestinal lumen.

By contrast, the trophozoites of intestinal eugregarines (e.g., lecudinids and septate gregarines) possess hundreds of epicytic folds that significantly increase surface area. This increase in surface area is advantageous for a greater reliance on surface-mediated nutrition within host intestinal systems and corresponds with the loss of both the apical complex (e.g., the conoid) and myzocytosis in trophozoites. However, increased surface sulcation confers increased cell rigidity, which limits the range of cellular deformation. Unlike archigregarines, intestinal eugregarines lack layers of longitudinal microtubules beneath the inner-membrane complex and, instead, utilise an actinomyosin-based system of gliding that is very different from the bending movements found in archigregarines (Mellor & Stebbings 1980; Heintzelman 2004). The gliding motility enables the trophozoites to find syzygy partners and position themselves in optimal environments within the intestinal lumen of the host. Nutrients are pushed across the trophozoite surface via undulating epicytic folds that alternate in position between straighter epicytic folds

(Vivier 1968; Vávra & Small 1969; Heller & Weise 1973; Leander *et al*. 2003b).

Transformations associated with the evolution of gregarine trophozoites are perhaps best reflected in the molecular phylogenetic relationships of the three *Selenidium* species studied so far (Fig. 6). A clade of two environment sequences, namely AY179975 (CCA38) and AY179976 (CCI31), appear to be closely related to *Selenidium* species, but so far no reference taxon is available to identify them at the cellular level. Nonetheless, the ultrastructural features of these as yet undescribed trophozoites should shed considerable light onto the origins of longitudinal folds and other gregarine characteristics. The trophozoites of *S. terebellae* are spindle-shaped, possess 4–6 longitudinal folds and appear to have a well-developed apical complex (Leander *et al*. 2003b). The spindle-shaped trophozoites of *S. serpulae* possess 19–23 longitudinal folds, which might reflect a greater dependency on surface-mediated nutrition. *Selenidium serpulae* is also closely related to a bizarre archigregarine that inhabits the intestines of *Phascolosoma agassizii* (the banded sipunculid), namely *S. vivax*. Mature trophozoites of *S. vivax* are large, tape-like cells (120–500 μm long) that are highly motile (Gunderson & Small 1986; Leander 2006). The longitudinal folds of *S. vivax* are unusual in being inconspicuous and transient, depending on the stage in cellular deformation (Gunderson & Small 1986; Leander *et al*. 2003b; Leander 2006). Thus, the sister relationship between *S. serpulae* and *S. vivax* demonstrates that the highly derived trophozoites in the latter lineage evolved from an ancestor having a trophozoite morphology much like that found in *S. terebella* and *S. serpulae* (e.g., spindle-shaped and a few longitudinal folds) (Fig. 6). The highly derived features of *S. vivax* also helps illustrate that archigregarines as a whole should not be considered 'primitive' and that the diversification of *Selenidium*-like parasites is probably more extensive than usually assumed.

Comparative morphology and molecular phylogenetic analyses suggest that transverse striations are a general feature of *Selenidium* and *Selenidium*-like species, such as *D. oweni*, *Meroselenidum keilini*, *S. pendula*, *S. potamillae*, S. *sabellariae* and *S. spionis* (Ray 1930; MacKinnin & Ray 1933; Schrével 1970; Dyson *et al*. 1993). *Selenidium vivax* possesses fine, but prominent transverse folds that are nearly identical in morphology and distribution to those described here for *S. serpulae*. The transverse striations on the trophozoites of *S. terebellae* are broader and less prominent than those found in *S. serpulae* and *S. vivax*, and are more evenly distributed over the cell surface (Leander *et al*. 2003b). Nonetheless, this shared character is not only concordant with the molecular phylogenetic results, but might represent a key synapomorphy for an emerging archigregarine clade or perhaps the plesiomorphic condition for a more inclusive apicomplexan clade (e.g., all gregarines or all apicomplexans).

The multimembranous structure, subgroove position and abundance of pinocytotic vesicle (syn. lipochondria) in *S. serpulae* are consistent with those described in other gregarines (Vivier & Schrével 1964; MacGregor & Thomas 1965; Vivier 1968; Desportes & Théodoridès 1969; Schrével 1971a; Desportes 1974; Hoshide & Todd 1996). The transverse structure of the peduncles leading to the pinocytotic vesicles, consisting of two parallel membranes orientated perpendicularly to the longitudinal axis of the grooves (Figs 4C,D and 5F), has not been described elsewhere in gregarines. However, I suspect that this structure was unnoticed in previous studies rather than being a novel feature of *S. serpulae*. The inconspicuous 'whorled structure' shown in Fig. 2D is enigmatic and without any homologue in other described apicomplexans. Other multiple-bound organelles, such as apicoplasts and nuclear blebs surrounded by a cisterna of endoplasmic reticulum, were not evident. 'Nuclear vacuoles', like that observed in *S. serpulae* (Fig. 4A), have also been described in other archigregarines, such as *M. keilini* (MacKinnin & Ray 1933), but the functional significance of these vacuoles is unknown. The vacuolated coat around the periphery of the nuclear envelope in *S. serpulae* appears to be novel (Figs 2D and 4B) and is most similar to the less prominent vacuolar layer lying beneath the nuclear envelope in *S. vivax* (Leander 2006). Moreover, the lobed nucleus in *S. serpulae* is also reminiscent of the nuclear structure described in *S. vivax* (Leander 2006), which reinforces the sister relationship between these two lineages recovered in SSU rDNA phylogenies (Fig. 6).

Archigregarines in the deep sea

The oocysts of archigregarines appear to be broadly distributed throughout marine sediments and are commonly ingested by invertebrate hosts that employ modes of nutrition involving deposit feeding and suspension feeding (e.g., tube worms, phoronids, sipunculids, errant polycheates and tunicates). Interestingly, the SSU rDNA sequence from *S. serpulae* was very closely related to sequences derived from an environmental PCR survey of a hydrothermal vent in the Gulf of California, namely C1-E017 (AY046619) and C2-E016 (AY046806). This molecular phylogenetic result suggests that archigregarines with a morphology and lifecycle much like that in *S. serpulae* are thriving in this oxygen poor ecosystem. In fact, the ubiquity of parasites in deep-sea environments has been one of the primary insights gained from environmental PCR surveys (Moreira & Lopez-Garcia 2003).

The close relationship between *S. serpulae* and the hydrothermal vent sequences is entirely consistent with the ultrastructural data described here. For instance, *S. serpulae* appears to possess inconspicuous mitochondria, which might reflect the reduction of these organelles during the evolution of this lineage. Mitochondrial reduction has occurred several

times independently during the course of eukaryotic evolution, especially in single-celled parasites (e.g., *Cryptosporidium*, microsporidia and trichomonads). The condition in *S. serpulae* is indicative of anaerobic metabolism, which might have enabled this lineage of parasites to survive as the host migrated into deeper oceanic environments. To the best of my knowledge, all other described gregarines possess conspicuous mitochondria, and the mitochondria of certain species, such as *S. vivax* and *S. hollandei*, are highly developed, arranged superficially and appear to play an important role in the rapid and continuous generation of ATP needed to support highly dynamic cellular deformations (Schrével 1971a; Leander 2006). The sister relationship between *S. serpulae* (reduced mitochondria) and *S. vivax* (developed mitochondria) suggests that the lack of mitochondria in *S. serpulae* represents an independent evolutionary transformation and is not homologous with the similar condition found in the putative gregarine relative *Cryptosporidium* (Riordan *et al*. 1999; Leander *et al*. 2003a, 2003b; Henriquez *et al*. 2005). Nonetheless, increased taxon sampling from archigregarines using both ultrastructural data and molecular markers should continue to shed considerably more light onto the biogeographical distribution and early evolutionary stages of the apicomplexan radiation.

Acknowledgements

This work was supported by grants from the National Science and Engineering Research Council of Canada (NSERC 283091–04) and the Canadian Institute for Advanced Research, Program in Evolutionary Biology. I am grateful to Kevin Wong for participating in the collection of host animals and isolation of parasites for DNA extraction.

References

Berney, C., Fahrni, J. & Pawlowski, J. (2004). How many novel eukaryotic 'kingdoms'? Pitfalls and limitations of environmental DNA surveys. *BMC Biology*, *2*, 1–13.

Beyer, T. V., Svezhova, N. V., Radchenko, A. I. & Sidorenko, N. V. (2002). Parasitophorous vacuole: morphofunctional diversity in different coccidian genera (A short insight into the problem). *Cell Biology International*, *26*, 861–871.

Bruno, W. J., Socci, N. D. & Halpern, A. L. (2000). Weighted neighbor joining: a likelihood-based approach to distance-based phylogeny reconstruction. *Molecular Biology and Evolution*, *17*, 189–197.

Carreno, R. A., Martin, D. S. & Barta, J. R. (1999). *Cryptosporidium* is more closely related to the gregarines than to coccidia as shown by phylogenetic analysis of apicomplexan parasites inferred using small-subunit ribosomal RNA gene sequences. *Parasitology Research*, *85*, 899–904.

Cavalier-Smith, T. (2004). Only six kingdoms of life. *Proceedings of the Royale Society of London B*, *271*, 1251–1262.

Cavalier-Smith, T. & Chao, E. E. (2004). Protalveolate phylogeny and systematics and the origins of Sporozoa and dinoflagellates (Phylum Myzozoa nom. nov.). *European Journal of Protistology*, *40*, 185–212.

Cox, F. E. G. (1994). The evolutionary expansion of the sporozoa. *International Journal for Parasitology*, *24*, 1301–1316.

Dawson, S. C. & Pace, N. R. (2002). Novel kingdom-level eukaryotic diversity in anoxic environments. *Proceedings of the National Academy of Sciences USA*, *99*, 8324–8329.

Deng, M., Rutherford, M. S. & Abrahamsen, M. S. (2004). Host intestinal epithelial response to *Cryptosporidium parvum*. *Advances in Drug Delivery Reviews*, *56*, 869–884.

Desportes, I. (1974). Ultrastructure et evolution nucléaire des trophozoïtes d'une grégarine d'ephéméroptère: *Enterocystis fungoides* M. Codreanu. *Journal of Protozoology*, *21*, 83–94.

Desportes. I. & Théodoridès, J. (1969). Ultrastructure of the gregarine *Callynthrochlamys phronimae* Frenzel; comparative study of its nucleus with that of *Thalicola salpae* (Frenzel) (Eugregarina). *Journal of Protozoology*, *16*, 449–460.

Dyson, J., Grahame, J. & Evennett, P. J. (1993). The mucron of the gregarine *Digyalum oweni* (Protozoa, Apicomplexa), parasitic in a *Littorina* species (Mollusca, Gastropoda). *Journal of Natural History*, *27*, 557–564.

Felsenstein, J. (1993). *PHYLIP (Phylogeny Inference Package)*. Seattle: University of Washington.

Grassé, P.-P. (1953). Classe des grégarinomorphes (Gregarinomorpha, N. nov., Gregarinae Haeckel, 1866; gregarinidea Lankester, 1885; grégarines des auteurs). In P. -P. Grassé (Ed.) *Traité de Zoologie* (pp. 590–690). Paris: Masson.

Gunderson, J. & Small, E. B. (1986). *Selenidium vivax* n. sp. (Protozoa, Apicomplexa) from the sipunculid *Phascolosoma agassizii* Keferstein, 1867. *Journal of Parasitology*, *72*, 107–110.

Heintzelman, M. B. (2004). Actin and myosin in *Gregarina polymorpha*. *Cell Motility and the Cytoskeleton*, *58*, 83–95.

Heller, G. & Weise, R. W. (1973). A scanning electron microscope study on *Gregarina* sp. from *Udeopsylla nigra*. *Journal of Protozoology*, *20*, 61–64.

Henriquez, F. L., Richards, T. A., Roberts, F., McLeod, R. & Roberts, C. W. (2005). The unusual mitochondrial compartment of *Cryptosporidium parvum*. *Trends in Parasitology*, *21*, 68–74.

Hoshide, K. & Todd, K. S. (1996). The fine structure of cell surface and hair-like projections of *Filipodium ozakii* Hukui 1939 Gamonts. *Acta Protozoologica*, *35*, 309–315.

Huelsenbeck, J. P. & Ronquist, F. (2001). MrBayes: bayesian inference of phylogenetic trees. *Bioinformatics*, *17*, 754–755.

Kuvardina, O. N. & Simdyanov, T. G. (2002). Fine structure of syzygy in *Selenidium pennatum* (Sporozoa, Archigregarinida). *Protistology*, *2*, 169–177.

Kuvardina, O. N., Leander, B. S., Aleshin, V. V., Mylnikov, A. P., Keeling, P. J. & Simdyanov, T. G. (2002). The phylogeny of colpodellids (Eukaryota, Alveolata) using small subunit rRNA genes suggests they are the free-living ancestors of apicomplexans. *Journal of Eukaryotic Microbiology*, *49*, 498–504.

Leander, B. S. (2006). Ultrastructure of the archigregarine *Selenidium vivax* (Apicomplexa) — a dynamic parasite of sipunculid worms (Host: *Phascolosoma agassizii*). *Marine Biology Research*, *2*, 178–190.

Leander, B. S. & Keeling, P. J. (2003). Morphostasis in alveolate evolution. *Trends in Ecology and Evolution*, *18*, 395–402.

Leander, B. S. & Keeling, P. J. (2004). Early evolutionary history of dinoflagellates and apicomplexans (Alveolata) as inferred from hsp90 and actin phylogenies. *Journal of Phycology*, *40*, 341–350.

Leander, B. S., Clopton, R. E. & Keeling, P. F. (2003a). Phylogeny of gregarines (Apicomplexa) as inferred from SSU rDNA and beta-tubulin. *International Journal of Systematic and Evolutionary Microbiology*, *53*, 345–354.

Leander, B. S., Harper, J. T. & Keeling, P. J. (2003b). Molecular phylogeny and surface morphology of marine aseptate gregarines (Apicomplexa): *Lecudina* and *Selenidium*. *Journal of Parasitology*, *89*, 1191–1205.

Leander, B. S., Kuvardina, O. N., Aleshin, V. V., Mylnikov, A. P. & Keeling, P. J. (2003c). Molecular phylogeny and surface morphology of *Colpodella edax* (Alveolata): insights into the phagotrophic ancestry of apicomplexans. *Journal of Eukaryotic Microbiology*, *50*, 334–340.

Leander, B. S., Lloyd, S. A. J., Marshall, W. & Landers, S. C. (2006). Phylogeny of marine gregarines (Apicomplexa) — *Pterospora*, *Lithocystis* and *Lankesteria* — and the origin (s) of coelomic parasitism. *Protist*, *157*, 45–60.

Levine, N. D. (1971). Taxonomy of the Archigregarinorida and Selenidiidae (Protozoa, Apicomplexa). *Journal of Protozoology*, *18*, 704–717.

Levine, N. D. (1976). Revision and checklist of the species of the aseptate gregarine genus *Lecudina*. *Transactions of the American Microscopical Society*, *95*, 695–702.

Levine, N. D. (1977a). Checklist of the species of the aseptate gregarine family Urosporidae. *International Journal for Parasitology*, 7, 101–108.

Levine, N. D. (1977b). Revision and checklist of the species (other than *Lecudina*) of the aseptate gregarine family Lecudinidae. *Journal of Protozoology*, *24*, 41–52.

MacGregor, H. C. & Thomas, P. A. (1965). The fine structure of two archigregarines, *Selenidium fallax* and *Ditrypanocystis cirratuli*. *Journal of Protozoology*, *12*, 438–443.

MacKinnin, D. L. & Ray, H. N. (1933). The life cycle of two species of *Selenidium* from the polychaete worm *Potamilla reniformis*. *Parasitology*, *25*, 143–167.

Maddison, D. R. & Maddison, W. P. (2000). *Macclade*. Sunderland, MA: Sinauer Associates, Inc.

Mellor, J. S. & Stebbings, H. (1980). Microtubules and the propagation of bending waves by the archigregarine, *Selenidium fallax*. *Journal of Experimental Biology*, *87*, 149–161.

Moreira, D. & Lopez-Garcia, P. (2003). Are hydrothermal vents oases for parasitic protists? *Trends in Parasitology*, *19*, 556–558.

Omoto, C. K., Toso, M., Tang, K. & Sibley, L. D. (2004). Expressed sequence tag (EST) analysis of gregarine gametocyst development. *International Journal for Parasitology*, *34*, 1265–1271.

Posada, D. & Crandall, K. A. (1998). MODELTEST: testing the model of DNA substitution. *Bioinformatics*, *14*, 817–818.

Ray, H. N. (1930). Studies on some protozoa in polychaete worms. I. Gregarines of the genus *Selenidium*. *Parasitology*, *22*, 370–400.

Riordan, C. E., Langreth, S. G., Sanchez, L. B., Kayser, O. & Keithly, J. S. (1999). Preliminary evidence for a mitochondrion in *Cryptosporidium parvum*: phylogenetic and therapeutic implications. *Journal of Eukaryotic Microbiology*, *46*, 52S–55S.

Schrével, J. (1968). L'ultrastructure de la région antérieure de la grégarine *Selenidium* et son intérêt pour l'étude de la nutrition chez les sporozoaires. *Journal de Microscopie*, 7, 391–410.

Schrével, J. (1970). Contribution a l'étude des Selenidiidae parasites d'annélides polychètes. I. Cycles biologiques. *Protistologica*, *6*, 389–426.

Schrével, J. (1971a). Contribution a l'étude des Selenidiidae parasites d'annélides polychètes. II. Ultrastructure de quelques trophozoïtes. *Protistologica*, 7, 101–130.

Schrével, J. (1971b). Observations biologique et ultrastructurales sur les Selenidiidae et leurs conséquences sur la systématique des grégarinomorphes. *Journal of Protozoology*, *18*, 448–470.

Schrével, J. & Philippe, M. (1993). The gregarines. In J. P. Krier & J. R. Baker (Eds) *Parasitic Protozoa*, 4, 133–245. Academic Press, San Diego.

Stebbings, H., Boe, G. S. & Garlick, P. R. (1974). Microtubules and movement in the archigregarine, *Selenidium fallax*. *Cell Tissue Research*, *148*, 331–345.

Strimmer, K. & Von Haeseler, A. (1996). Quartet Puzzling: a quartet maximum likelihood method for reconstructing tree topologies. *Molecular Biology and Evolution*, *13*, 964–969.

Swofford, D. L. (1999). *Phylogenetic Analysis Using Parsimony (and Other Methods)* PAUP* *4.0*. Sunderland, MA: Sinauer Associates, Inc.

Théodoridès, J. (1984). The phylogeny of the Gregarinia. *Origin of Life*, *13*, 339–342.

Vávra, J. & Small, E. B. (1969). Scanning electron microscopy of gregarines (Protozoa, Sporozoa) and its contribution to the theory of gregarine movement. *Journal of Protozoology*, *16*, 745–757.

Vivier, E. (1968). L'organization ultrastructurale corticale de la gregarine *Lecudina pellucida*: ses repports avec l'alimentation et la locomotion. *Journal of Protozoology*, *15*, 230–246.

Vivier, E. & Schrével, J. (1964). Étude, au microscope électronique, d'une grégarine du genre *Selenidium*, parasite de *Sabellaria alveolata* L. *Journal de Microscopie*, *3*, 651–670.

Vivier, E. & Schrével, J. (1966). Les ultrastructures cytoplasmiques de *Selenidium hollandei*, n. sp. grégarine parasite de *Sabellaria alveolata* L. *Journal de Microscopie*, *5*, 213–228.

Wray, C. G., Langer, M. R., DeSalle, R., Lee, J. J. & Lipps, J. H. (1995). Origin of the foraminifera. *Proceedings of the National Academy of Sciences USA*, *92*, 141–145.

Zhu, G., Keithly, J. S. & Philippe, H. (2000). What is the phylogenetic position of *Cryptosporidium*? *International Journal of Systematic and Evolutionary Microbiology*, *50*, 1673–1681.

